Strongly correlated electron materials. II. Band structure and renormalized density of states in heavy-fermion systems and high-T_c superconductors

J. Costa-Quintana, F. López-Aguilar, and L. Puig-Puig
Departament de Física, Grup d'Electromagnetisme, Universitat Autònoma de Barcelona, Bellaterra, E-08193 Barcelona, Spain
(Received 4 March 1992; revised manuscript received 27 January 1993)

We give a method for obtaining renormalized electronic structures arising from quasiparticle band structures of actual Hubbard systems, using some of the self-energies deduced in paper I of this series. The quasiparticle band structures are determined from an appropriate modification of the augmented plane-wave method, and the renormalized density of states is found from the spectral functions. We calculate the quasiparticle structure of a Ce system, which presents the three characteristic types of resonances of the pseudogap regime mentioned in paper I of this series and also the electronic structure of Y-Ba-Cu-O, which seems to display the characteristics of a standard Fermi liquid or a marginal Fermi liquid.

I. INTRODUCTION

Two of the most characteristic Hubbard systems are the cubic Laves phase of Ce alloys, which belongs to the f-system group,[1,2] and $YBa_2Cu_3O_{7-x}$,[3] which is the best known and studied high-T_c superconductor. The objective of this paper is to give an answer to the question of what they have in common and what their differences are from the quasiparticle structure point of view. We pose these questions because both apparently different systems are treated and analyzed from the same Hamiltonian model. The analysis of the conditions within the Hubbard model which lead to the quasiparticle structure of these systems has contributed towards clarifying some points of their respective phenomenologies. In this paper, we consider that the different Hubbard systems consist of interacting particles which occupy single-particle states with an experimentally detected Fermi surface. The self-energies used in this calculation are deduced in paper I of this series (henceforth referred to as I) and we determine here the density of states from the spectral functions, considering the renormalization factor and the half-life of the quasistates of both the α phase of $CeAl_2$ and the $YBa_2Cu_3O_7$ system in the normal-state phase.

The strongly correlated electrons, in both $CeAl_2$ and $YBa_2Cu_3O_7$, can be studied by means of a sea of quasiparticles whose properties are determined from an energy-dependent self-energy acting in single bands.[2,4] The measurements of the de Haas–van Alphen effect, performed in heavy-fermion systems[5] five years ago, and the precise x-ray-photoemission data with angle resolution realized recently in high-T_c superconductors[6] suggest that there are, in both cases, well-defined Fermi surfaces. The option in which the Hubbard systems are considered as a quasiparticle sea whose states arise from the hybridization of strongly correlated orbitals with other extended states is thus justified.

The determination of the electronic structures of these materials needs as a first step the calculation of the spectrum and wave functions of their quasiparticle sea. This is performed by using the self-energies deduced in I [Eqs. (21) and (26) of I] and solving the respective Schrödinger-like equations [Eq. (29) of I]. The second step is the determination of the density of states (DOS) calculated from the spectral functions. This DOS is deduced by considering the half-life and the renormalization factor of the quasistates obtained in the first step. One point which is extensively analyzed in I is that for values close to the total occupation or the total unoccupation of n_m (i.e., $n_m \to 0$ or $n_m \to 1$) and/or for sufficiently large bandwidths, the above-mentioned self-energy can yield interacting systems in the Fermi liquid or marginal Fermi liquid regime.[7] In terms of the self-energy analysis performed in I, this regime implies that the number of peaks in the spectral function of the quasiparticle system is equal to the number of stationary states of the noninteracting system. In contrast, for n_m values close to the half-occupation and for sufficiently narrow bandwidths, the self-energy yields the three characteristic resonances: the lower, middle, and upper resonances (these cases are called the pseudogap regime[7]). α-$CeAl_2$ and $YBa_2Cu_3O_7$ have been chosen for two reasons. First, the quasiparticle electronic structures of these two systems are interesting by themselves. Second, each of these materials belongs to a different group with respect to the form of the spectral functions of the interacting systems, since α-$CeAl_2$ is a clear case of the "pseudogap regime" and $YBa_2Cu_3O_7$ can be classified in the group which contains one resonance for stationary state.

II. BAND METHOD AND RENORMALIZED DOS

The analytical expression of the self-energy deduced in I [Eqs. (21) and (26) of that paper] is used in this paper for obtaining the band structure and the DOS of both α-$CeAl_2$ and $YBa_2Cu_3O_7$. The Schrödinger-like equa-

0163-1829/93/48(2)/1139(9)/$06.00 ©1993 The American Physical Society

tion that is necessary to solve to obtain the quasiparticle structure of the interacting system is

$$\left[-\nabla^2 + V^n_{\mathrm{MT}}(\mathbf{r})\right]\varphi_{\mathbf{k}\alpha}(\mathbf{r}) + \int \Sigma'(\mathbf{r},\mathbf{r}',E_{\mathbf{k}\alpha})\varphi_{\mathbf{k}\alpha}(\mathbf{r}')\,d^3r' = E_{\mathbf{k}\alpha}\varphi_{\mathbf{k}\alpha}(\mathbf{r}). \quad (1)$$

The real part of $E_{\mathbf{k}\alpha}$ is the $\varepsilon_{\mathbf{k},\alpha}$ spectrum. This spectrum corresponds to states which contain several l orbitals, and only the strongly correlated m component of each state experiences the effects of $\Sigma(\mathbf{r},\mathbf{r}',\omega)$. Each m symmetry is shifted by an energy $\mathrm{Re}\Sigma_m(\omega)$, and each $\varepsilon_{\mathbf{k},\alpha}$ state is shifted by an energy approximately equal to $[\mathrm{Re}\Sigma_m(\varepsilon_{\mathbf{k},\alpha})]\,n_m(\varepsilon_{\mathbf{k},\alpha})$, where $n_m(\varepsilon_{\mathbf{k},\alpha}) = |\langle \mathbf{k}\alpha|m\rangle|^2$.

We solve (1) using the augmented plane-wave (APW) method, and the resulting matrix elements of the secular equation, considering the self-energy operator, are

$$\left[M^\alpha_{ij}(E)\right]_{\Sigma'} = \left[M^\alpha_{ij}(E)\right]_{\mathrm{APW}} + \sum_R X^{\alpha R}_j \sum_\nu Y^{\nu R}_{ij} \sum_m Z^{\nu R}_{ij,m}(E), \quad (2)$$

where $\left[M^\alpha_{ij}(E)\right]_{\mathrm{APW}}$ are the standard APW matrix elements corresponding to the irreducible representation α and

$$X^{\alpha R}_j = (4\pi)^2 \frac{g}{n_\alpha}\Gamma^\alpha_{11}(R)\exp(i\mathbf{K}_j\cdot\mathbf{t}_R), \quad (3)$$

$$Y^{\nu R}_{ij} = \frac{S^2_\nu}{\Omega}\exp\left[i(R^{-1}\mathbf{K}_j - \mathbf{K}_i)\cdot\mathbf{r}_\nu\right], \quad (4)$$

$$Z^{\nu R}_{ij,m}(E) = I_m(K_iS_\nu)I_m(K_jS_\nu) \times \sum_t^{2m+1}\left[\frac{d}{dr}\ln\frac{\chi_m(\epsilon_t,r)}{\chi_m(E,r)}\right]_{r=S_\nu} \times\phi^\nu_t(\mathbf{K}_i)\phi^\nu_t(R^{-1}\mathbf{K}_j), \quad (5)$$

with

$$\epsilon_t = E - \mathrm{Re}\Sigma_t(E), \quad (6)$$

where g is the number of symmetry operations of the group corresponding to the vector $\mathbf{k}$; n_α is the dimension of the irreducible representation α with matrix elements Γ^α; $\mathbf{K}_j = \mathbf{k} + \mathbf{G}_j$ ($\mathbf{G}_j$ is a reciprocal lattice vector); $\mathbf{t}_R$ is the nonprimitive lattice vector associated with the symmetry operation R (in the case of a symmorphic symmetry group $\mathbf{t}_R = 0$ for all R); the index ν runs over the m-electron atoms pertaining to the primitive cell; S_ν is the muffin-tin radius of the ν atom whose position vector is $\mathbf{r}_\nu$; $\phi^\nu_t(\mathbf{K}_j)$ are linear combinations of $l = m$ orbitals compatible with the crystal symmetry and centered on the ν-electron atom; Ω stands for the primitive cell volume; I_m is the m spherical Bessel function; $\chi_m(\epsilon,r)$ is the radial part of the $l = m$ orbital calculated for the ϵ energy from the Schrödinger radial equation obtained within the APW. The second term of the right-hand side of (2) can be interpreted as the equivalent pseudopotential arising from the self-energy operator between two ij APW bases. The band-structure calculation described by Eqs. (2)–(6) is general for any self-energy functional whenever this comes from a Hubbard Hamiltonian.

The E energies that satisfy the condition

$$\det\left[M^\alpha_{ij}(E)\right]_{\Sigma'} = 0 \quad (7)$$

are eigenvalues which correspond to the eigenstates with a fixed $\mathbf{k}$ vector and α symmetry. On the other hand, the variable E in (7) is related to ϵ_t by (6). Thus, the difference $E - \epsilon_t$ derives from the self-energy effects. When one finds an eigenvalue E of the interacting Hubbard system, the corresponding ϵ_t is an energy of the noninteracting system. This means that ϵ_t is located around the divergence of the logarithmic derivative of the function $\chi_m(\epsilon,r)$ evaluated at $r = S_\nu$ and deduced with the Hamiltonian $[-\nabla^2 + V^n_{\mathrm{MT}}(\mathbf{r})]$.

This band-calculation method presents some similarities with other previous methods recently published[8] which consider orbital polarization effects. However, our method includes the orbital polarization effects in the strongly correlated states by means of a (energy-dependent) dynamic potential, and it is at this key point that it differs from the above-mentioned methods of Ref. 8, which introduce these effects by static potentials.

The DOS of the interacting system is determined by

$$\mathcal{N}(\omega) = \frac{1}{\pi}\sum_{\mathbf{k}\alpha} A(\varepsilon_{\mathbf{k}\alpha}) \quad (8)$$

and

$$A(\varepsilon_{\mathbf{k}\alpha}) = \frac{\gamma_{\mathbf{k}\alpha}}{(\omega - \varepsilon_{\mathbf{k}\alpha} - \delta_{\mathbf{k}\alpha})^2 + \gamma^2_{\mathbf{k}\alpha}}, \quad (9)$$

where $\delta_{\mathbf{k}\alpha} \simeq \sum_m \mathrm{Re}\Sigma_m(\varepsilon_{\mathbf{k}\alpha})|\langle \mathbf{k}\alpha|m\rangle|^2$ and $\gamma_{\mathbf{k}\alpha} \simeq \sum_m \mathrm{Im}\Sigma_m(\varepsilon_{\mathbf{k}\alpha})|\langle \mathbf{k}\alpha|m\rangle|^2$. The imaginary part of the self-energy causes the $|\mathbf{k}\alpha\rangle$ states to become quasiparticle states, and their half-life can be approximately calculated by $\tau^{-1}_{\mathbf{k}\alpha} = \gamma_{\mathbf{k}\alpha}$.

For values of ω for which $\mathrm{Re}\Sigma_m(\omega)$ is small and/or does not vary much, Eq. (9) is given by

$$A(\varepsilon_{\mathbf{k}\alpha}) = Z(\varepsilon_{\mathbf{k}\alpha})\frac{Z(\varepsilon_{\mathbf{k}\alpha})\gamma_{\mathbf{k}\alpha}}{(\omega - \varepsilon_{\mathbf{k}\alpha})^2 + [Z(\varepsilon_{\mathbf{k}\alpha})\gamma_{\mathbf{k}\alpha}]^2}, \quad (10)$$

where $Z(\varepsilon_{\mathbf{k}\alpha})$ is the renormalization factor of the quasistate $\varphi_{\mathbf{k}\alpha}$ corresponding to the Green's-function pole. We have found that this factor $Z(\varepsilon_{\mathbf{k}\alpha})$, corresponding to a self-energy functional like that used in this paper, can be written as

$$Z(\varepsilon_{\mathbf{k}\alpha}) = \left[\left|1 - \sum_m n_m(\omega)\frac{\partial\mathrm{Re}\Sigma_m(\omega)}{\partial\omega}\right|_{\omega=\varepsilon_{\mathbf{k}\alpha}}\right]^{-1}. \quad (11)$$

On the other hand, it is well known that the effective mass is

$$\frac{m_{\mathrm{eff}}}{m_0} \approx Z^{-1}(\varepsilon_{\mathbf{k}\alpha}). \quad (12)$$

Therefore, m_{eff}/m_0 depends on the $\Sigma_m(\omega)$ variations versus ω, and on $n_m(\omega)$. If one only considers a first-order self-energy,[9] then m_{eff}/m_0 is 1. In the f-electron case

described in this paper, $m_{\rm eff}/m_0$ has sharp peaks in the energy interval where the three structures arising from the partially occupied m symmetry appear. Therefore, the specific heat, which depends on $m_{\rm eff}$, will be large. This property is an experimental feature which characterizes the heavy-fermion compounds.

The summation (8) is obtained by dividing the irreducible Brillouin zone (IBZ) into tetrahedra. In each tetrahedron, we consider that the energies of the quasistates $\varepsilon_{\mathbf{k}\alpha}$ vary linearly. Then, $\mathcal{N}(\omega)$ is given by

$$\mathcal{N}(\omega) = \frac{1}{V\pi} \sum_i \int dk_{i\|}\, \overline{A_i}(k_{i\|}) S(k_{i\|}) \qquad (13)$$

where $\overline{A_i}(k_{i\|})$ is the average value of the $A(\varepsilon_{\mathbf{k}\alpha})$ function in a constant-energy plane within the ith tetrahedron, and $S(k_{i\|})$ is the surface of the intersection of this plane with the given tetrahedron. The index i runs over all tetrahedra of the IBZ, V is the volume of the IBZ, and $k_{i\|}$ is the component of the quasimomentum $\mathbf{k}$ parallel to the gradient $\nabla\varepsilon_{\mathbf{k}\alpha}$ within the ith tetrahedron.

III. RESULTS ON α-$CeAl_2$

This Ce compound has been analyzed from several points of view, and there is a general consensus on the following features of its electronic structure.

(i) At low temperature, it presents a light heavy-fermion state with a γ coefficient for the electronic specific heat $\simeq$150 mJ/(mol f atom K^2) (see Meisner *et al.* in Ref. 10), this γ being $\simeq$15 times larger than, for instance, that of the α-Ce element. This implies that the quasistates at energies close to E_F suffer large self-energy effects in such a way that their respective renormalization factors are reduced considerably.

(ii) One of the most striking features of its electronic structure is that all studies of x-ray photoemission spectroscopy (XPS) detect an f structure at E_F and another one at about 2.5 eV below E_F (see, for instance, Allen *et al.* and Croft *et al.*[1]). Furthermore, the inverse photoemission spectroscopy (IPS) performed by bremsstrahlung isocromat radiation[11] detects in the Ce systems two f structures, one of them just above E_F and another giant f structure at $\simeq$4 eV above E_F. Therefore, this compound presents an f structure with four peaks, which is clearly very different from what is obtained with the local-density formalism calculations.

(iii) The n_f occupation (see Gunnarsson *et al.*[1]), deduced by either XPS or IPS, is close to 0.8, and the symmetry of the occupied orbital is most probably the XYZ.

As a consequence of this experimental properties, we see that α-$CeAl_2$ is a heavy-fermion compound which presents an f splitting, and that has one partially occupied f orbital which is clearly hybridized with other extended states arising from the Al. It therefore corresponds to the group of strongly correlated compounds whose interacting system of quasiparticles presents renormalized DOS with f structures corresponding to the pseudogap regime (i.e., there are three resonances for each state of the noninteracting system[7]). The model described in paper I and in the preceding sections of this paper can be easily understood by its application to this case, because here the noncorrelated states close to E_F do not hide the f resonances, and its heavy-fermion character is clearly manifested. On the other hand, we have chosen the α phase of $CeAl_2$ because it presents Pauli paramagnetism (see, for instance, Allen *et al.*[1]) and therefore the splittings of the f bands below and/or above E_F are caused by the U correlation effects. These splittings cannot be attributed to either spin-polarization effects or to any other cause, except the dynamics of the Hubbard Hamiltonian. The spin-polarization effects might be considered as an explanation for some features of the f structures in the γ phase of $CeAl_2$, which is antiferromagnetic. However, also in this phase the f splitting below E_F was detected by Allen *et al.* and Croft *et al.* (see Ref. 1) by direct x-ray photoemission and they concluded that the value of this f splitting in α-$CeAl_2$ is equal to that of γ-$CeAl_2$. In addition, the analysis of the γ-α transition of the Ce compounds reveals that, due to the hybridization, the f occupation of the α phase presents a slight decrease with respect to that of the γ phase, but their f electronic structures remain the same under hydrostatic pressure. Therefore, these two experimental facts invalidate the explanation of the spin-polarization effects in both the α and the γ phase of this compound.

The structure of multiple f peaks in the electronic structure of the Ce compounds has also been studied extensively from a theoretical point of view.[2,12,13] Three of these f peaks, shown in Figs. 1 and 2, correspond to the partially occupied f orbital, and the giant fourth f peak corresponds to the six totally unoccupied f symmetries. The mechanism for which the self-energy (1) produces

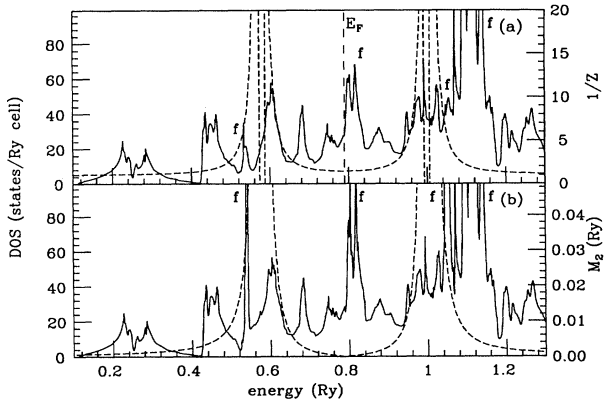

FIG. 1. (a) DOS of α-$CeAl_2$ considering the RPA to the dielectric function and $U_f = 0.5$ Ry. The f peaks are marked with an f. The dashed line represents the inverse of the renormalization factor for f states without hybridization, i.e., $1 - \partial\Sigma_m(\omega)/\partial\omega$, and the scale of the right-hand side corresponds to this renormalization function. (b) Density of levels (i.e., considering a renormalization factor equal to the unity and an infinite half-life) within the RPA approximation to the dielectric function, and the same U_f. The dashed line represents the absolute value of the imaginary part of the self-energy [$M_2(\omega) = {\rm Im}\Sigma_m$] and the energy scale on the right-hand side concerns this M_2 function.

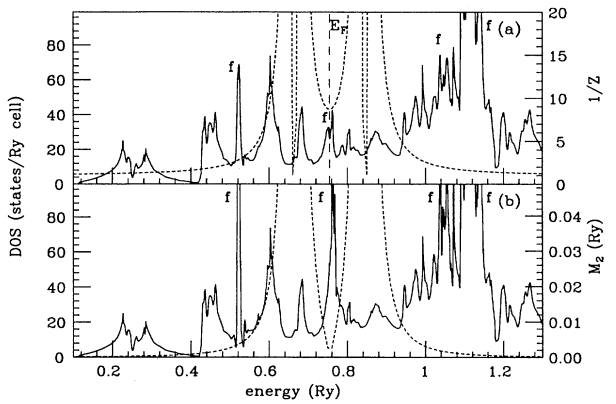

FIG. 2. Same as Fig. 1, but considering the calculation performed with the ERPA dielectric function.

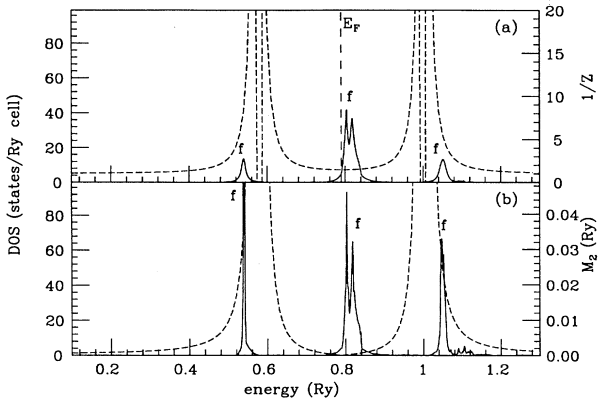

FIG. 3. fDOS of the partially occupied orbital of the calculation of Fig. 1. The three peaks correspond to the first three peaks of this figure. The dashed lines have the same meaning as in Fig. 1.

this multiple f structure can be understood in the light of the argument given in Secs. V and VI of paper I. There we explain that in the pseudogap regime there are three f resonances in the interacting system for each f band of stationary states in the noninteracting system. In addition, each of these resonances can hybridize with other extended states, producing the formation of hybridization pseudogaps as in Fig. 1.

A first calculation is performed considering a random-phase approximation (RPA) to the dielectric function, and the results for the DOS are shown in Fig. 1(a). In Fig. 1(b), we give the density of levels (DOL), these being considered as stationary states (i.e., having an infinite half-life) whose renormalization factor is 1. Therefore, in the DOL calculation, the corresponding spectral functions $A(\varepsilon_{\mathbf{k}\alpha})$ are $\delta(\omega - \varepsilon_{\mathbf{k}\alpha})$. This calculation is performed in order to show the effects, in the DOS, of the renormalization factor and the quasiparticle character of the spectrum deduced by Eqs. (2)–(7). The renormalization factor, the dashed line in Fig. 1(a), and the imaginary part of the self-energy, the dashed line in Fig. 1(b), cause a decrease of the heights of the f peaks of the DOS with respect to those of the DOL curve. The imaginary part of the self-energy allows us to fix E_F of the interacting system. In Fig. 2 we perform a similar calculation to that of Fig. 1, but using the extended random-phase approximation (ERPA) for the dielectric function. The most significant difference between these two calculations is the double structure of the second f peak of Fig. 1 close to E_F.

In Figs. 3 and 4, we show the results of the partial density of f electrons (fDOS) corresponding to the orbital whose symmetry is XYZ in the RPA and ERPA, respectively; the three peaks visible in these figures correspond to the three first f peaks of the analogous plot of Figs. 1 and 2 for the total DOS. The results of Figs. 3(a) and 4(a) are obtained from the actual spectral function [i.e., considering Eq. (9)] while Figs. 3(b) and 4(b) are obtained considering a δ Dirac spectral function for each eigenvector deduced by Eq. (1). From the comparison of these groups of figures, the effect produced by the imaginary part of the self-energy is evident. We also see that Figs. 3(a) and 4(a) present a similar pattern to that outlined in paper I for the general cases in the pseudogap regime. The pseudogap in the resonance just at E_F of Fig. 4(a) is so narrow that it does not appear in the figure. We want to recall that these results are obtained using the non-self-consistent self-energy [Eq. (26) of paper I]. We could carry out the self-consistent process for the self-energy using the calculated DOS of Fig. 1(a) or 2(a) in Eq. (23) of paper I. However, this self-consistent process, in a realistic case, needs much computational work whose realization does not seem justified since we are not sure that it would yield to sufficient improvements in the results to compensate the necessary consumption of CPU time.

The DOS of Figs. 1 and 2 show a similar electronic structure with the following main features: (i) E_F is located at the second f peak. This characteristic appears in all available $CeAl_2$ experimental data—see, for

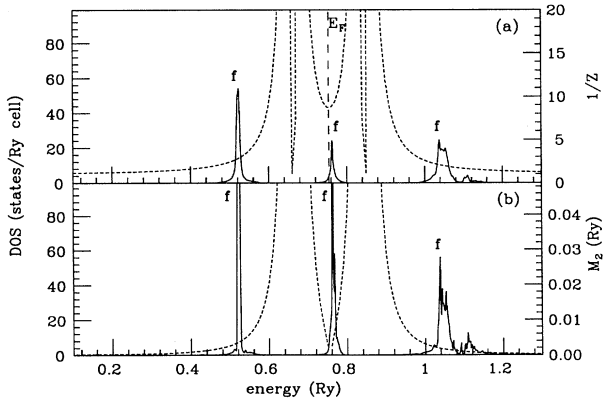

FIG. 4. fDOS of the partially occupied orbital of the calculation of Fig. 2. The three peaks correspond to the first three peaks of this figure. The dashed lines have the same meaning as in Fig. 1.

instance, Allen *et al.* and Croft *et al.* in Ref. 1. (ii) The first f peak lies approximately 3 eV below E_F (see also Allen *et al.* and Croft *et al.*). (iii) The third resonance corresponding to the partially occupied orbital is located just below the giant f peak arising from the other totally empty f symmetries. (iv) The fourth f peak is approximately 4 eV above E_F. These two latter features can be observed by IPS (see, for instance, Wuilloud *et al.* in Ref. 11). Therefore, the self-energies used in these calculations yield results which are qualitatively and quantitatively in reasonable agreement with XPS and IPS measurements.[1,11]

The self-energy effects have a great influence, via the renormalization factor, in the heavy-fermion state, whose features (specific heat, Kondo temperature, electrical and thermical behavior, possible superconducting transition, etc.) depend on the f resonances close to E_F. The value of the renormalized linear coefficient of the specific heat γ^* is clearly enhanced, given that the average of the renormalization factor for energies close to E_F is such that $Z^{-1} \simeq 35$ for the ERPA self-energy, and this is in reasonable agreement with the results of the experimental specific heat. This agreement concerning the results of the renormalization factor is more modest in the case of the RPA self-energy, since this approximation yields $Z^{-1} \simeq 2.5$, which is far from the experimental result.

The existence of the double f structure at E_F (see Fig. 1) could be related to the conduction properties of the material. Joyce *et al.*[1] have detected this double f structure just below E_F in several Ce compounds ($CeSi_2$, $CeSb_2$, etc.), and they have concluded that this is caused by a screening channel. This is coherent with the explanation that we give for the existence of this feature in α-$CeAl_2$ since it appears because of a dynamic screening of the U interaction and the corresponding self-energy effects. However, the exact location of the double structure in the vicinity of E_F is dependent on the material since this location is strongly dependent on the f count as well as on the magnetic behavior, which can be different for each Ce compound. In our calculation this middle double structure is just above E_F. On the other hand, in Figs. 1–4, the sign change of $\mathrm{Im}\Sigma$ coincides with the Fermi level, which in these figures is determined by the integral of the DOS, thus satisfying the necessary condition for the Luttinger theorem to be fulfilled.

The Stoner enhancement factor F_S is a characteristic variable of the Ce systems which has great relevance in the heavy-fermion state.[14] This factor[15] ($F_S = [1 - Un_f^2\mathcal{N}_f(E_F)]^{-1}$) and the static pairing potential for some types of heavy-fermion superconductors [$V_0 = -\frac{1}{2}Un_f^2F_S$ (Refs. 14 and 15)] are dependent on the middle structure at E_F. This structure is double (split by a narrow pseudogap) both in $CeRu_2$ and in $CeOs_2$,[15] and the different location of E_F and the different values of $\mathcal{N}_f(E_F)$ in these compounds can be the reason why the pairing potential V_0 produces a superconducting transition in the first case and not in the second. In the case of $CeAl_2$, the band parameters [$\mathcal{N}_f(E_F)$, n_f and U] do not allow superconducting behavior by means of this pairing potential, since the partial fDOS at E_F implies a repulsive V_0. A superconducting transition in $CeAl_2$ would require high hydrostatic pressures for varying $\mathcal{N}_f(E_F)$.

In summary, we have given a calculation of the DOS of an actual case, obtained from a quasiparticle band structure determined by an energy-dependent potential appropriated for strongly correlated systems, whose characteristics are those of a heavy-fermion system.

IV. RESULTS ON $YBa_2Cu_3O_7$

The special features of the normal-state electronic structure of the $YBa_2Cu_3O_7$ compound are the key to the high-T_c superconductivity of the $YBa_2Cu_3O_{7-x}$ systems. It is well accepted that the normal state of this compound can be described as an interacting quasiparticle sea with a perfectly well-defined Fermi surface.[16] Strongly correlated states and band states with large $E(\mathbf{k})$ dispersion coexist in an energy interval of approximately 6 eV around the Fermi level.[6] Moreover, the $d_{x^2-y^2}$ orbitals of Cu2 and p_x/p_y of O2/O3 largely overlap, this overlap being slightly larger than that found in the Cu1 and O4/O1 atoms[17] (Cu2, O2, and O3 atoms belong to the CuO_2 sheets and Cu1, O4, and O1 are in the linear CuO_3 chain). This latter condition produces a sufficiently large bandwidth to almost reduce to the static terms [$U(X - n_m)$] the self-energies deduced in I [Eqs. (23) and (26) of paper I]. We would like to emphasize that there is a term $U(X - n_m)$ for each m-strongly correlated symmetry of each atom, so the different n_m occupations bring about the possibility of splitting between the different bands arising from the different m orbitals. In addition, it is worth remembering that the existence of only static terms in the self-energy leads to an interacting quasiparticle gas whose spectral functions present only the middle strongly correlated resonance (see Secs. V and VI of paper I). In this case, the enhancement of the effective masses is less than that of the pseudogap regime and therefore the heavy-fermion state is not possible. The relatively small values of the specific heat of $YBa_2Cu_3O_7$ are in agreement with the practically null effective-mass enhancement obtained with the self-energy in this case.

We present in this calculation the electronic structure of $YBa_2Cu_3O_7$ obtained by the method described in Eqs. (2)–(7), which includes different Coulomb correlation effects for the p and d orbitals according to their occupations in the different atoms. The Coulomb correlation effects produce a selective orbital polarization in the different Cu and O atoms according to the occupation of their orbitals. The calculated electronic structure of $YBa_2Cu_3O_7$ is compatible with the photoemission experimental results.[18]

We include the spectrum of the ground state of the noninteracting system in the $YBa_2Cu_3O_7$ system for obtaining the self-energy used in (1). With this self-energy, we calculate the spectrum of the interacting system. This point constitutes the most important difference between this calculation and our former calculations of the electronic structure of this compound,[19] since in previous papers we took into account the state occupation of each $p(d)$ orbital in the most extreme features of this ground state. These conditions were to consider unoccupied a d orbital of Cu1, a p orbital of O4, and another p orbital

of O1.

Results on the electronic structure, without considering Coulomb correlation effects, have been previously published in recent papers,[19] and the main features of these results are the following [see Fig. 5(b)]: (i) The Fermi level lies $\simeq$0.7 eV above the gravity center of the giant $3d$ structure of Cu2; (ii) the $2p$ bands are located in the whole energy interval of the conduction band; and (iii) there is no pseudogap in the density of states of the $2p$ oxygen and $3d$ copper bands. We present these results in this paper to compare them to the DOS of the interacting system. In Fig. 5(a), we plot the total DOS considering U_p and U_d different from zero, and its main features are the following.

(i) The Fermi level is approximately 3 eV above the giant peak of the valence band corresponding to $3d$ states of Cu2. This result is a clear improvement with respect to that obtained by the local-density formalism (LDF) since the LDF calculations locate the gravity center of these Cu2 $3d$ states around 2 eV above those obtained by photoemission spectroscopies (see for instance Johnson *et al.*[18]).

(ii) E_F is located close to a zone of the DOS with a relatively small $\mathcal{N}(E_F)$ value [see in Fig. 5(a) the pseudogap at energies close to 0.1 Ry below E_F]. This pseudogap (quasigap) is produced by the hybridization along with the strong-correlation effects. The existence of this pseudogap has been schematically proposed in other recent works (see Mahan, Martin, and Satpathy; Kim, Levin, and Auerbach;[3] and Varma[20]) and implies that a semiconducting phase can be obtained for increasing values of x in $YBa_2Cu_3O_{7-x}$ close to the superconducting transition. The existence of this pseudogap leads to a decrease in the distribution of the density of quasiparticles, which is an essential condition for the appearance of high-T_c superconductivity.[3,20] This pseudogap tends to approach E_F for increasing x values in $YBa_2Cu_3O_{7-x}$, since when increasing x there are more O4/O1 vacancies, and therefore the strong-correlation gap increases due to the enhancement of the electron localization in the O4/O1 and Cu1 atoms.[17] One of the main causes for the appearance of this quasigap is clearly the Coulomb correlation effect contained in the self-energy (1) deduced from the U energy. The LDF calculations, without considering this self-energy, are not able to obtain this pseudogap in the total DOS just by hybridization effects. Besides, this pseudogap is a true gap in some partial DOS (see Figs. 6 and 7). The tendency of the gap to increase, and the gradual approximation of E_F to this gap, when one increases x, is compatible with the experimental fact that $YBa_2Cu_3O_{7-x}$ tends towards a Mott antiferromagnetic insulator for integral values of the hole number per atom of the CuO_2 planes (i.e., for $x \rightarrow 1$).[17] Evidently, these former reasons are valid in the supposed case where the rigid-band type of approach for the bands and the self-energy can also be valid. For the bands, the small number of the unoccupied states due to the doping (between 0.4 and 0.8 electron states per primitive cell) with respect to number of electrons (68 per primitive cell) of these systems leads one to consider that the DOS is almost unchanged by these amounts of doping. For the self-energy, the point is not so clear. However, for the bandwidths arising from the p and d orbitals involved in the strong correlation self-energy, the influence of the occupation of these orbitals in the self-energy is less important than that corresponding to the bandwidths. Therefore, small variations of the occupations of these orbitals due to the doping yield, in these conditions, small differences in the self-energy effects.

(iii) The structures in the DOS above the gap (in Fig. 5) are an admixture of $3d$ Cu1/Cu2 and $2p$ O1/O2/O3/O4 states in the symmetries, which can be seen in Figs. 6 and 7. At E_F, there is an admixture of all orbitals which can also be seen in Figs. 6 and 7.

From inspection of the partial DOS given in Figs. 6 and 7, we deduce that (i) the gravity center of the $3d_{xz}$, $3d_{xy}$, $3d_{yz}$, and $3d_{3x^2-r}$ bands of Cu1 of the CuO_3 chain are around 5 eV below E_F and are clearly formed by localized and strongly correlated states. This fact is in

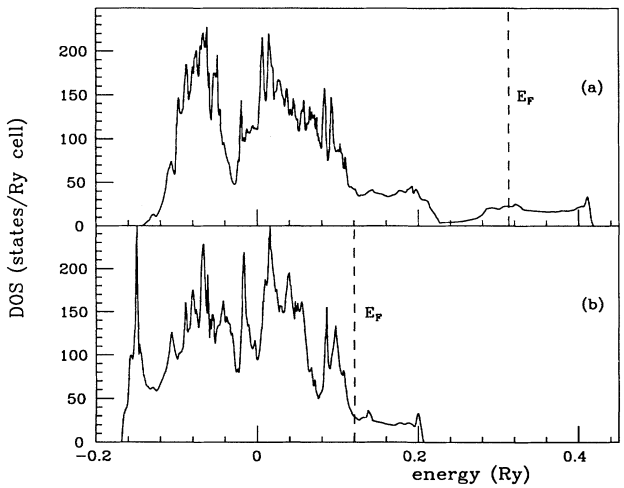

FIG. 5. DOS of $YBa_2Cu_3O_7$. (a) Considering U_d=0.26 Ry and U_p=0.22 Ry in the expression of the self-energy. (b) Considering $U_d = U_p = 0$.

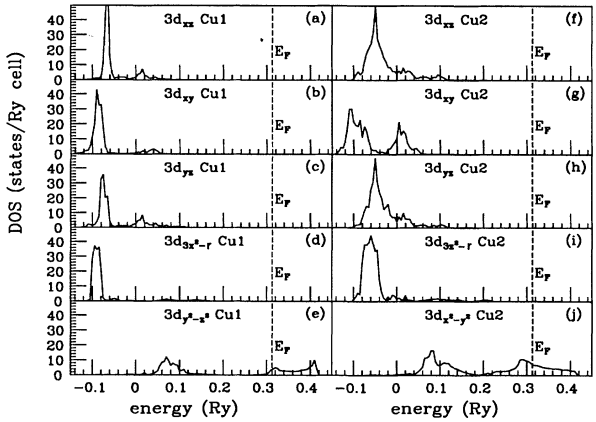

FIG. 6. Partial dDOS of Cu1 and Cu2 of $YBa_2Cu_3O_7$ considering $U_d = 0.26$ Ry and $U_p = 0.22$ Ry.

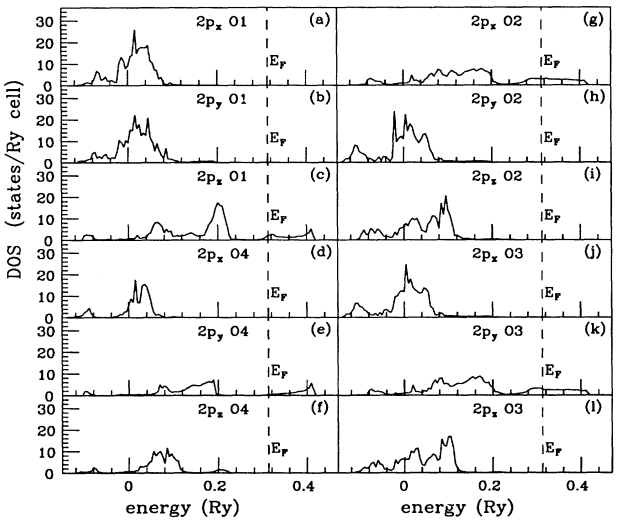

FIG. 7. Partial pDOS of all O atoms with $U_d = 0.26$ Ry and $U_p = 0.22$ Ry.

agreement with the spectroscopy results of Takahashi *et al.*[6] In contrast, the $3d_{y^2-z^2}$ band is less correlated than the above-mentioned bands and is approximately half-occupied. In addition, the occupied zone is split from the unoccupied one by an hybridization gap of about 3 eV. (ii) The holes of oxygen atoms of the CuO_3 chain are located in the $2p_z$ and $2p_y$ bands of the O1 and O4 atoms, respectively. The hybridization of these bands with the $3d_{y^2-z^2}$ of Cu1 produces the splitting of this latter band. (iii) The $3d_{xz}$, $3d_{xy}$, $3d_{yz}$, and $3d_{3z^2-r}$ bands of Cu2 are also correlated, but less than the same symmetries corresponding to the chain. The $3d_{x^2-y^2}$ bands of these same atoms are clearly hybridized with the $2p_x$ ($2p_y$) bands of the O2 (O3) atoms. This hybridization yields larger bandwidths than those of the other bands of the CuO_2 sheets and is responsible, along with the correlation effects, for the existence of holes in these planes. (iv) The different occupation of each band implies different strongly correlated effects produced by the self-energy, and the locations of their gravity centers are shifted according to their respective n_m. All these features of our results on the electronic structure of $YBa_2Cu_3O_7$ are in reasonable agreement with the experimental results given in Refs. 17 and 18, and satisfy the requirement of other theoretical models.[3,20]

In our results, the holes in symmetries $d_{x^2-y^2}$ of Cu2 and p_x/p_y of O2/O3 cause ionization states approximately equal to +1.3 for Cu2 and approximately equal to −1.8 for O2/O3. Therefore, the number of holes is 0.7 and 0.2 per Cu2 and O2/O3, respectively. These results correspond to $YBa_2Cu_3O_7$, which is not a superconductor. For oxygen compositions between 6.6 and 6.8, the superconductivity appears, and it seems that these vacancies are almost exclusively produced from oxygen atoms of the type O4. These vacancies imply a larger localization of the p and d states of the chain with respect to those of the sheets with the same orbital symmetries.[17,19] Therefore, for minimization of the total energy of the system, the two electrons per vacancy which remain in the crystal[19] have the tendency to go toward the sheets. As a consequence, the vacancies can produce slight, but nonvanishing, decreases in the hole density of the atoms Cu2 and O2/O3 of the CuO_2 sheets. It is complex to perform a quantitative estimation of this mechanism if one does not dispose of quantitative experimental results of the symmetries of the holes and their evolution with the variations of the x parameter. However, this speculation seems possible and even probable.

The hole states have a large interatomic overlapping and the corresponding interatomic hole-hole interaction undergoes a strong dynamic screening.[20,21] A dynamically screened interaction for these holes can be given by[21] $\mathbf{V}(\omega) = [\mathbf{I} - \mathbf{U}\mathbf{\Pi}(\omega)]^{-1}\,\mathbf{U}$, where $\mathbf{V}$ and $\mathbf{U}$ are matrices defined in the $p \otimes d$ space, and $\mathbf{\Pi}$ is a diagonal matrix whose elements are the polarizations,[21] which can be calculated by similar procedures to those of paper I. The dependence on $\mathbf{k}$ of the $\mathbf{V}$ interaction could provide the evaluation of the anisotropy of the superconducting gap. However, there is a certain experimental tendency to consider that the superconductivity in the CuO_2 planes is isotropic.[22,23] In the case of two bands (one p and the other d), the matrices of the equation which define the $\mathbf{V}$ pair potential have dimension 2, and its matrix elements are $V_{pp}(\omega)$, $V_{dd}(\omega)$, and $V_{pd}(\omega)$. The analysis of the various interatomic interactions can be performed in a similar way,[19,21] and their variations versus the band parameters present similar behaviors.[19,21] There is a sufficiently wide energy interval where these matrix elements can be attractive interactions for the case of the electronic structure of YBaCuO systems. Therefore, both V_{pp} and V_{dd}, along with V_{pd}, can produce coupling and superconductivity for determined band parameters, and the high-T_c superconductivity could be due to a combination of the three V interactions.

In paper I, we have introduced in the strong-coupling equations a coupling potential arising from the dielectric function (14) of that paper, considering one only m orbital. For the DOS of the superconducting phase of $YBa_2Cu_3O_{7-x}$, the above-mentioned screening produces attractive interaction at frequencies below a critical frequency, which is estimated to be around 0.3 eV.[22,24] The factor that can be decisive in the T_c is the type of screening used for obtaining the pair potential, but given a determined screening function, the main parameters that determine the hole-hole coupling are the location and width of frequency interval for which the pair potential is attractive. In all cases of screening, the location and width of this interval are strongly dependent on the band parameters (bandwidths, orbital occupation, DOS at E_F, and Coulomb correlation). It seems to be a result of many screening functions that the T_c deduced from the corresponding strong-coupling equations vary linearly on the product $U\mathcal{N}_0$. This implies that to maintain the same T_c, the p bands should have a larger value of $\mathcal{N}_0$ than the d bands, since these latter bands can present a U value larger than the p bands. Therefore, following the strong-coupling analysis of paper I, and the results of the partial DOS of Figs. 6 and 7, the most probable candidates to form the pairs are the $2p_y$ ($2p_x$) and $3d_{y^2-x^2}$

symmetries of the O3 (O2) and Cu1 atoms, respectively, since the band parameters of their partial DOS seem to be compatible with the required values for obtaining superconductivity. However, in order to have quantitative criteria for deciding what symmetries are more favorable for contributing to the superconductivity and to evaluate the physical variables of this superconductivity, it is precise to introduce several screening functions within the strong-coupling equations, this being one of our investigations in progress.

To sum up, our results on $YBa_2Cu_3O_{7-x}$ seem to be compatible with some experimental data and are characterized by the different types of the valence-band states, since there are strongly correlated states coexisting with band states. This implies an occupation in the external shells of the two-dimensional layers similar to that of the chain. However, the greater electronic localization in the chain compared to that of the planes causes the Coulomb correlation effects to be larger in the chain than in the planes. On the other hand, the strong-coupling theory applied to $YBa_2Cu_3O_7$ with the coupling potential $\mathbf{V}$, calculated with the band parameters deduced in this paper, may generate superconductivity, with T_c depending on the screening function used in the strong-coupling equations.

V. CONCLUDING REMARKS

In this paper, we have presented a method for analyzing the electronic structure in two different systems with different behaviors with respect to specific heat, spectroscopy, and superconductivity, but whose common point is that they clearly present strong-correlation effects in the electron quasistates of their conduction bands. In the case of α-$CeAl_2$, we obtain a renormalized DOS where the three different resonances of the so-called pseudogap regime appear clearly. Its singular electron spectroscopy pattern can be seen in our DOS curves and seems to be in reasonable qualitative and quantitative agreement with the direct and inverse XPS measurements. In addition, the large value for the specific heat is compatible with the self-energy and renormalized DOS deduced in this paper. Using the general model for the Hubbard systems, we have also determined the self-energy and renormalized DOS corresponding to $YBa_2Cu_3O_7$. The differences between the electronic structures of these two compounds are obtained with the same self-energy functional, but considering in each case the different bandwidths and occupations of their strongly correlated orbitals. Our results in $YBa_2Cu_3O_7$ seem to be in reasonable agreement with the experimental results of XPS spectroscopies and with the requirements of other theoretical models referring to these compounds. This agreement is in two essential points. First, the quasiparticle DOS near E_F shows a quasigap which is absent in the standard LDF band-structure calculation. This quasigap seems to be a necessary condition for the possible couplings to produce superconductivity. Second, the giant peaks of the total DOS are approximately 3 eV below E_F, which is in reasonable agreement with the XPS data, while the LDF band-structure calculation locates these peaks approximately 0.7 eV below E_F.

ACKNOWLEDGMENTS

This work has been financed by the CICYT (Research Projects Nos. MAT89-0675 and MAT91-0955) and the MIDAS program of Spain. One of us (L.P.P.) acknowledges financial support from the Ministerio de Educación y Ciencia of Spain.

[1]See, for instance, J.W. Allen, S.J. Oh, I. Lindau, J.M. Lawrence, L.J. Johansson, and S.B. Hagstrom, Phys. Rev. Lett. **46**, 1100 (1981); M. Croft, J.H. Weaver, D.J. Peterman, and F. Franciosi, *ibid.* **46**, 1104 (1981); O. Gunnarsson, K. Scönhammer, J.C. Fuggle, F.U. Hillebrecht, J.M. Esteva, R.C. Kasnatak, and B. Hillebrand, Phys. Rev. B **28**, 7330 (1983); G.R. Stewart, Rev. Mod. Phys. **56**, 755 (1984); F. Patthey, W.D. Schneider, Y. Baer, and B. Delley, Phys. Rev. Lett. **58**, 2810 (1987); P. Schlottmann, Phys. Rep. **181**, 3 (1989); J.J. Joyce, A.J. Arko, J. Lawrence, P.C. Canfield, Z. Fisk, R.J. Bartlett, and J.D. Thompson, Phys. Rev. Lett. **68**, 236 (1992).

[2]M.M. Steiner, R.C. Albers, D.J. Scalapino, and L.J. Sham, Phys. Rev. B **43**, 1637 (1991), and references therein.

[3]P.W. Anderson, Science **235**, 1196 (1987); J.H. Kim, K. Levin, and A. Auerbach, Phys. Rev. B **39**, 11 633 (1989); A.K. Mahan, R.M. Martin, and S. Satpathy, *ibid.* **38**, 6650 (1988); W.E. Pickett, Rev. Mod. Phys. **61**, 801 (1990).

[4]See, for instance, T.M. Rice, J. Magn. Magn. Mater. **63-64**, 689 (1987); J. Less Common Metals **164-165**, 1439 (1990).

[5]L. Taillefer and G.G. Lonzarich, Phys. Rev. Lett. **60**, 1570 (1988).

[6]T. Takahashi *et al.*, Phys. Rev. B **39**, 6636 (1989).

[7]A. Kampf and J.R. Schrieffer, Phys. Rev. B **41**, 6399 (1990); **42**, 7967 (1990).

[8]M.R. Norman, Phys. Rev. Lett. **64**, 1162 (1990); V.I. Anisimov, M.A. Korotin, and E.Z. Kurmaev, J. Phys. Condens. Matter **2**, 3973 (1990); A. Svane and O. Gunnarsson, Phys. Rev. Lett. **65**, 1148 (1990).

[9]F. López-Aguilar and J. Costa-Quintana, J. Phys. C **20**, 2485 (1986); S. Balle, J. Costa-Quintana, and F. López-Aguilar, *ibid.* **20**, L223 (1987); Phys. Rev. B **37**, 6615 (1988).

[10]F. Steglich, J. Magn. Magn. Mater. **63-64**, 694 (1987); G.P. Meisner, A.L. Giorgi, A.C. Lawson, G.R. Stewart, J.O. Willis, M.S. Wire, and J.L. Smith, Phys. Rev. Lett. **53**, 1829 (1984).

[11]Y. Baer, H.R. Ott, J.C. Fuggle, and L.F. de Long, Phys. Rev. B **24**, 5384 (1981); E. Wuillord, H.R. Moser, W.D. Scheneider, and Y. Baer, *ibid.* **28**, 7354 (1983); J.S. Kang, J.W. Allen, O. Gunnarsson, N.E. Christensen, O.K. Andersen, Y. Lasailly, M.B. Marple, and M.S. Torikachivili, *ibid.* **41**, 6610 (1990).

[12]See, for instance, R.M. Martin, Phys. Rev. Lett. **48**, 362 (1982); C. Czycholl, Phys. Rep. **143**, 277 (1986); P. Schlottmann, *ibid.* **181**, 3 (1989).

[13]V. Zlatic, S.K. Ghatak, and K.H. Benermann, Phys. Rev. Lett. **57**, 1263 (1986).
[14]P.W. Anderson, Phys. Rev. B **30**, 1549 (1984).
[15]F. López-Aguilar, S. Balle, and J. Costa-Quintana, Phys. Rev. B **38**, 163 (1988).
[16]A. Bansil, R. Pankaluoto, R.S. Rao, P.E. Mijnarends, W. Duglosz, R. Prasad, and L.C. Smedskjaer, Phys. Rev. Lett. **61**, 2480 (1988); J.C. Campuzano *et al.*, *ibid.* **64**, 2308 (1990).
[17]J. Ashkenazi and C.G. Kuper, Physica C **162-164**, 767 (1989); N. Nücker *et al.*, Phys. Rev. B **39**, 6619 (1989); E.E. Alp *et al.*, *ibid.* **40**, 9385 (1989); J.C. Campuzano *et al.*, Phys. Rev. Lett. **64**, 2308 (1990); P. Monthoux, Phys. Rev. B **41**, 11 128 (1990); Z. Schlesinger *et al.*, Phys. Rev. Lett. **65**, 801 (1990); Nature **343**, 242 (1990).
[18]P.D. Johnson *et al.*, Phys. Rev. B **35**, 8811 (1987); J.A. Yarmoff *et al.*, *ibid.* **36**, 3967 (1987); A.J. Viescas *et al.*, *ibid.* **37**, 3738 (1988); H. Rietschel *et al.*, Physica C **153-155**, 1067 (1988); K.C. Hass, Solid State Phys. **42**, 213 (1989); A.J. Arko *et al.*, Phys. Rev. B **40**, 2268 (1989).
[19]J. Costa-Quintana, F. López-Aguilar, S. Balle, and R. Salvador, Phys. Rev. B **39**, 9675 (1989); F. López-Aguilar and J. Costa-Quintana, *ibid.* **42**, 4150 (1990).
[20]C.M. Varma, J. Res. Dev. **33**, 215 (1989); C.M. Varma, S. Schmitt-Rink, and E. Abrahams, in *Novel Superconductivity*, edited by S.A. Wolf and W.Z. Kresin (Plenum, New York, 1987), p. 355.
[21]F. López-Aguilar, J. Costa-Quintana, and S. Balle, J. Less-Common Metals **164-165**, 1480 (1990); F. López-Aguilar and J. Costa-Quintana, Mod. Phys. Lett. B **5**, 1499 (1991).
[22]Z. Schlesinger *et al.*, Phys. Rev. Lett. **65**, 801 (1990); Nature **343**, 242 (1990).
[23]F. Mila and E. Abrahams, Phys. Rev. Lett. **67**, 2379 (1991); R. Combescot, *ibid.* **67**, 148 (1991).
[24]C.M. Varma *et al.*, Phys. Rev. Lett. **63**, 1996 (1989).